arXiv:1707.02211v1 [cs.DS] 7 Jul 2017

The Stellar tree: a Compact Representation for Simplicial Complexes and Beyond

Riccardo Fellegara, *University of Maryland, College Park (MD), USA*
Kenneth Weiss, *Lawrence Livermore National Laboratory, Livermore (CA), USA*
Leila De Floriani, *University of Maryland, College Park (MD), USA*

Abstract

The efficient representation and management of simplicial and cell complexes is an active research topic in several fields, including geometric modeling, computer graphics, scientific visualization, and geographic data processing. In this paper, we propose the *Stellar tree*, a topological data structure for performing efficient topological queries on simplicial and non-simplicial complexes. We prove that a *Stellar tree* provides a scalable, compact and flexible data structure to represent these complexes, using a *fraction* of the memory required by a corresponding topological data structure on the global complex.

1 Introduction

Efficient mesh data structures play a fundamental role in a broad range of mesh processing applications in computer graphics, geometric modeling, scientific visualization, geographic information systems, finite element analysis, and in data analysis and machine learning. Although simple problems can be easily modeled on small low dimensional meshes, phenomena of interest might only occur on much larger meshes and in higher dimensions. Thus, we often require flexibility to deal with increasingly complex meshes including those defined by irregularly connected heterogeneous and/or multidimensional cell types discretizing spaces with complicated topology. Moreover, as advances in computing capabilities continue to outpace those in memory, it becomes increasingly important to optimize and exploit the mesh locality as we process and locally query it. Such queries are the primary means of interacting with the mesh and have historically been posed in terms of a few spatial and topological primitives. However, while there are simple, intuitive models for representing polygonal surfaces, there are numerous challenges in generalizing these structures to higher dimensions and in scaling to large meshes.

In this paper, we first introduce the *Stellar decomposition*, a model for topological data structures that can efficiently navigate the topological connectivity of simplicial complexes and certain classes of cell complexes, e.g. those composed of quadrilaterals, polygons, hexahedra, prisms and pyramids. The defining property of a Stellar decomposition is that the complex is broken up into *regions*, where each region is a collection of vertices of the complex, and each vertex within a region has sufficient information to locally reconstruct its *star*, i.e., the set of cells from the complex that are incident in that vertex.

A Stellar decomposition is *general*, in that it can easily represent arbitrary complexes with a manifold or non-manifold domain, *scalable* to complexes both in high dimensions and with a large number of cells, and *flexible* in that it enables users to defer decisions about which topological connectivity relations to encode. It, therefore, supports the generation of optimal application-dependent local data structures at runtime. Due to the locality of successive queries in typical mesh processing applications, the construction costs of these local topological data structures are amortized over multiple mesh operations while processing a local region.

We introduce the *Stellar tree* as a concrete instance of the Stellar decomposition model. Stellar trees utilize a hierarchical nD-quadtree or kD-tree as decomposition and are easily *tunable* using a single parameter that defines the maximum number of vertices in each local region of the decomposition.

In this paper we present:

1. the formal theoretical definition of a Stellar decomposition that provides a solid base for several possible representations exploiting this type of decomposition;
2. the definition of a compact encoding for the entities indexed by each region of the decomposition;
3. the definition of a concrete spatio-topological representation of the Stellar decomposition, the *Stellar tree*. The decomposition in a Stellar tree is based on a hierarchical spatial index, and thus, the indexed complex is spatially embedded;
4. the description of the procedures for exploiting the spatial coherence of the indexed entities and for compressing the Stellar tree representation through a compact encoding;
5. the description of a generic paradigm that can be adopted by any application defined on top of the Stellar tree.

The remainder of this paper is organized as follow. In Sections 2 and 3, we review background notions and related work respectively. In Section 4, we provide the definition of Stellar decomposition, in which we define all the components of a Stellar decomposition, plus the mapping functions that define the relation between the indexed entities and the regions of the decomposition. Then, we describe the encoding of the complex and of the entities indexed by the regions of the decomposition. In Section 5, we give the definition of a spatio-topological representation defined on top of the Stellar decomposition, the Stellar tree, and then, the encoding of the hierarchical decomposition. In Section 6, we describe in details the algorithms defined to generate a Stellar tree and those that exploit the spatial locality of the indexed entities. In Section 7, we give a complete comparison between the Stellar tree and several *state-of-the-art* topological data structures for manifold and non-manifold complexes.

2 Background notions

In this section, we review notions related to cell and simplicial complexes, the basic combinatorial structures for representing discretized shapes. Throughout the paper, we use n to denote the dimension of the ambient space, d to represent the maximum dimension of the underlying complex and k to denote the dimension of a cell from the complex, where $0 \leq k \leq d$ and typically $d \leq n$.

A k-dimensional *cell* in the n-dimensional Euclidean space $\mathbb{E}^n$ is a subset of $\mathbb{E}^n$ homeomorphic to a closed k-dimensional ball $B^k = \{x \in \mathbb{E}^k : \|x\| \leq 1\}$. A d-dimensional *cell complex* Γ in $\mathbb{E}^n$ is a finite set of cells with disjoint interiors and of dimension at most d such that the boundary of each k-cell γ consists of the union of the other cells of Γ with dimension less than k. A cell which does not belong to the boundary of any other cell in Γ is called a *top cell*. Γ is a *pure* cell complex when all top cells have dimension d. The subset of $\mathbb{E}^n$ spanned by the cells of Γ is called the *domain* of Γ.

In this paper, we are concerned with a restricted class of cell complexes whose cells can be fully reconstructed by their set of vertices, e.g. via a canonical ordering [Schoof and Yarberry, 1994, Poirier et al., 1998, Remacle and Shephard, 2003, Tautges, 2010]. We refer to this class of complexes as *Canonical Polytope complexes (CP complexes)* and note that it includes simplicial complexes, cubical complexes, polygonal cell complexes and heterogeneous meshes with cells from the finite element 'zoo' (e.g. simplices, hexahedra, pyramids, and prisms).

A pair of cells in a CP complex Σ are *incident* if one is a face of the other and *h-adjacent* if they have the same dimension and are incident in a common h-face. We informally refer to vertices (0-cells) as *adjacent* if they are both incident in a common edge (1-cell) and, similarly, for k-cells that are incident in a common $(k-1)$-cell. The *(combinatorial) boundary* of a CP cell σ is defined by the set of its faces. The *star* of a CP cell σ, denoted $St(\sigma)$, is the set of its *co-faces*, i.e., CP cells in Σ that have σ as a face. The *link* of a CP cell σ, denoted $Lk(\sigma)$, is the set of all the faces of cells in $St(\sigma)$ that are not incident in σ. Two h-cells σ and σ' in Σ are *h-connected* if there is a sequence of $(h-1)$-adjacent h-cells in Σ from σ to σ'.

We can now define a d-dimensional *CP complex* Σ as a set of CP-cells in $\mathbb{E}^n$ of dimension at most d such that:

1. Σ contains all CP-cells in the boundary of the CP-cells in Σ;
2. the intersection of any two CP-cells in Σ is *conforming*, i.e., it is either empty or a shared face of both CP-cells.

Simplicial complexes are an important subset of CP complexes whose cells are all *simplices*. Let k be a non-

negative integer. A k-simplex σ is the convex hull of $k+1$ independent points in $\mathbb{E}^n$ (with $k \leq n$), called vertices of σ. A *face* of a k-simplex σ is an h-simplex ($0 \leq h \leq k$) generated by $h+1$ vertices of σ.

Another important notion is that of a *(combinatorial) manifold*. A subset M of the Euclidean space $\mathbb{E}^n$ is called a *d-manifold*, with $d \leq n$, if and only if every point of M has a neighborhood homeomorphic to the open d-dimensional ball. For CP complexes, this corresponds to the condition that the link of every vertex is a combinatorial $(d-1)$-sphere, which becomes an undecidable problem for $d > 4$ [Nabutovsky, 1996]. A more practical concept for the purpose of representing CP complexes is that of pseudo-manifold. A pure CP complex is *pseudo-manifold* when its top cells are all d-connected and its $(d-1)$-cells are incident in at most two d-cells. Informally, we refer to the connected and compact subspace of $\mathbb{E}^n$ not satisfying the manifold conditions as *non-manifold*.

Queries on a cell complex are often posed in terms of *topological relations* defined by the adjacencies and incidences of its cells. Let us consider a CP complex Σ and a k-cell $\sigma \in \Sigma$, with $0 \leq k \leq d$:

- a *boundary relation* $R_{k,p}(\sigma)$, with $0 \leq p < k$, consists of the p-cells of Σ in the boundary of σ;
- a *co-boundary relation* $R_{k,q}(\sigma)$, with $k < q \leq n$, consists of the q-cells of Σ in the star of σ;
- an *adjacency relation* $R_{k,k}(\sigma)$ consists of the set of k-cells of Σ that are adjacent to σ.

3 Related work

In this section, we review the state of the art on topological mesh data structures and hierarchical spatial indexes.

3.1 Topological mesh data structures

There has been much research on efficient representations for manifold cell and simplicial complexes, especially for the 2D case (see [De Floriani and Hui, 2005] for a comprehensive survey of topological data structures for manifold and non-manifold shapes).

A topological mesh data structure over a cell complex encodes a subset of its topological relations and supports the efficient reconstruction of the local topological connectivity over its elements. Topological data structures can be classified according to: (i) the *dimension* of the cell complex, (ii) the *domain* to be approximated, i.e., manifolds, pure and non-pure shapes, non-manifold shapes, (iii) the subset of topological information directly encoded, and (iv) the *organization* of topological information directly encoded, i.e., explicit or implicit data structures. The explicit cells and connectivity relations can either be allocated on demand using small local structures, or contiguously, e.g. using arrays. In the former case, pointers are used to reference the elements, which can be useful when the data structure needs to support frequent updates to the underlying cells or their connectivity. In the latter case, indexes of the cells within the array can be used to efficiently reference the elements.

Broadly speaking, topological data structures can be categorized as *incidence-based* or *adjacency-based* representations. Whereas incidence-based data structures primarily encode their topological connectivity through incidence relations over all cells in the complex, adjacency-based data structures primarily encode their connectivity through adjacency relations over the top cells of complex.

The *Incidence Graph* (*IG*) [Edelsbrunner, 1987] is the prototypical incidence-based data structure for arbitrary shapes discretized by cell complexes in arbitrary dimension. The IG explicitly encodes all cells of a given cell complex Γ, and for each p-cell γ, its immediate boundary and co-boundary relations (i.e., $R_{p,p-1}$ and $R_{p,p+1}$). Several compact representations with the same expressive power as the IG have been developed for simplicial complexes [De Floriani et al., 2004, De Floriani et al., 2010], which typically require less than half the storage space as the IG [Canino and De Floriani, 2014]. Perhaps the most common incidence-based data structure for polygonal 2-complexes is the *half-edge* data structure [Mantyla, 1988], which encodes the incidences among edges, their bounding vertices, and co-bounding faces. *Combinatorial maps* [Lienhardt, 1994, Damiand and Lienhardt, 2014] generalize this notion to higher dimensions.

A more compact alternative provided by an *Indexed data structure* [Lawson, 1977] which explicitly encodes only vertices, top cells and the boundary relations from top cells to their vertices. Since the cells of a CP complex are entirely determined by their ordered list of vertices, this provides sufficient information to efficiently extract all boundary relations among the cells, but not the co-boundary or adjacency relations. The *Indexed data*

structure with Adjacencies (IA) [Paoluzzi et al., 1993, Nielson, 1997] extends the indexed representation to manifold simplicial complexes of arbitrary dimension by explicitly encoding adjacency relation $R_{d,d}$, leading to an adjacency-based representation. All remaining topological relations can be efficiently recovered if we also encode a single top simplex in the star of each vertex (i.e., a subset of relation $R_{0,d}$).

The *Corner-Table (CoT)* data structure [Rossignac et al., 2001] is also an adjacency-based data structure. It is defined only for conforming triangle meshes, where it has the same representational power as the IA data structure. It uses *corners* as a conceptual abstraction to represent individual vertices of a triangle and encodes topological relations among corners and their incident vertices and triangles. The *Sorted Opposite Table (SOT)* data structure [Gurung and Rossignac, 2009] extends the Corner-Table data structure to tetrahedral meshes and introduces several storage optimizations. Most notably, the SOT is able to reconstruct boundary relation $R_{d,0}$ from co-boundary relations $R_{0,d}$ (implicitly encoded) and $R_{d,d}$ relations (explicitly encoded), reducing the SOT's topological overhead by nearly a factor of two. Since modifications to the mesh require non-local reconstructions of the associated data structures, this representation is suitable for applications in which the mesh is static.

The *Generalized Indexed data structure with Adjacencies (IA* data structure)* [Canino et al., 2011] extends the representational domain of the IA data structure to non-manifold and mixed dimensional simplicial complexes. The IA* data structure is compact, in the sense that it gracefully degrades to the IA data structure in locally manifold neighborhoods of the mesh, and has been shown to be more compact than incidence-based data structures, especially as the dimension increases [Canino and De Floriani, 2014].

The Simplex tree [Boissonnat and Maria, 2014] also encodes general simplicial complexes of arbitrary dimension. It explicitly stores all simplices of the complex within a *trie* [Fredkin, 1960] whose nodes are in bijection with the simplices of the complex. An analysis in [Fugacci et al., 2015] indicates that the IA* data structure (provided by the *Mangrove TDS* library [MTDSL, 2014]) is 10-30% more compact than a lightweight Simplex tree implementation (provided by the *GUDHI* library [GUDHI, 2016] without co-boundary relations).

The *Skeleton-Blocker* data structure [Attali et al., 2012] encodes simplicial complexes that are close to *flag complexes* (simplicial complexes whose cells are entirely determined from the structure of the 1-skeleton) and has been successfully employed for executing edge contractions on such complexes. It encodes the 1-skeleton and the *blockers*, simplices that are not in Σ, but whose faces are. Its generation procedure is computationally intensive for general simplicial complexes since it has to insert simplices of all dimensions in order to identify the *blockers*.

We compare the Stellar tree representation with the IA, CoT, and SOT data structures as well as the Simplex tree, and IA* data structures in Section 7.3.

3.2 Hierarchical spatial indexes

A spatial index is a data structure used for indexing spatial information, such as points, lines or surfaces in the Euclidean space. Spatial indexes form a decomposition of the embedding space into *regions*. This can be driven by: 1. an *object-based* or a *space-based* criterion for generating the decomposition. 2. an *organization* of the regions, i.e., using a *hierarchical* or a *non-hierarchical* (*flat*) organization. The two characteristics are independent, and thus, for example, we can have hierarchical object-based decompositions, as well as flat space-based ones.

We now consider how the regions of a decomposition can intersect. In an *overlapping* decomposition the intersection between the regions can be non-empty on both the interiors and on the boundary of their domain, while, in a *non-overlapping* decomposition intersections can only occur on domain boundaries. We say that a region is *nested* within another region if it is entirely contained within that region. In the remainder of this section, we focus on *hierarchical spatial indexes*, which can be classified by the dimensionality of the underlying ambient space and by the types of entities indexed.

Hierarchical spatial indexes for point data are provided by *Point Region (PR)* quadtrees/octrees and kD-trees [Samet, 2006]. In these indexes, the shape of the tree is independent of the order in which the points are inserted, and the points are only indexed by leaf blocks. The storage requirements of these structures can be reduced by allowing leaf blocks to index multiple points, as in the

bucket PR quadtree/octree [Samet, 2006], whose *bucketing threshold* determines the number of points that can be indexed by a leaf block before it is refined.

Several data structures have been proposed for spatial indexing of *polygonal maps (PM)*, including graphs and planar triangle meshes. *PM quadtrees* [Samet and Webber, 1985] extend the PR quadtrees to represent polygonal maps considered as a structured collection of edges. While there are several variants (PM_1, PM_2, PM_3 and the randomized *PMR)*, which differ in the criterion used to refine leaf blocks, all maintain within the leaf blocks a list of intersecting edges from the mesh. The *PM_2-Triangle quadtree* [De Floriani et al., 2008] specializes PM quadtrees over triangle meshes and has been applied to terrain models. The PM index family has also been extended to *PM octrees* encoding polyhedral objects in 3D [Carlbom et al., 1985, Navazo, 1989, Samet, 2006], where the subdivision rules have been adjusted to handle edges and polygonal faces of the mesh elements. In [De Floriani et al., 2010], we have developed a collection of spatial indexes for tetrahedral meshes, that we call *Tetrahedral trees*.

We note that data structures in the PM family are *spatial data structures* optimized for efficient spatial queries on a complex (e.g., point location, containment and proximity queries) and are not equipped to reconstruct the connectivity of the complex. In contrast, the *PR-star octree* [Weiss et al., 2011] is a topological data structure for tetrahedral meshes embedded in 3D space. It augments the bucket PR octree with a list of tetrahedra incident in the vertices of its leaf blocks, i.e., those in the *star* of its vertices. This data structure has been shown to be effective with geometrical and topological applications including local curvature estimation, mesh validation and simplification [Weiss et al., 2011], morphological feature extraction [Weiss et al., 2013] and morphological simplification [Fellegara et al., 2014].

In this paper, we have generalized the PR-star data structure to handle a broader class of complexes (CP complexes) in arbitrary dimensions and with an arbitrary domain (i.e., non-manifold and non-pure complexes). At the same time, our new leaf block encoding further exploits the spatial coherence of the mesh, yielding a significant storage saving compared to PR-star trees (see Section 7.2).

Other approaches utilize a spatial index to reduce the memory requirements for out-of-core or memory intensive mesh processing. [Cignoni et al., 2003b] introduce an external memory spatial data structure for triangle meshes embedded in $\mathbb{E}^3$. Whereas, our aim is to enable efficient topological operations on the elements of general simplicial and CP complexes, the objective of [Cignoni et al., 2003b] is to support compact out-of-core processing of massive triangle meshes. Since their data structure is dimension-specific, exploiting geometric and topological properties of triangle meshes in $\mathbb{E}^3$, it would be difficult to generalize to more general CP complexes and to higher dimensions. [Dey et al., 2010] use an octree to index a large triangle mesh for localized Delaunay remeshing. Due to the significant overhead associated with their computations, their octrees are typically shallow, containing very few octree blocks. [Cignoni et al., 2003a, Cignoni et al., 2004] associate patches of triangles with the simplicial regions of a multiresolution diamond hierarchy [Weiss and De Floriani, 2011] for interactive rendering and visualization of triangulated terrains and polygonal models.

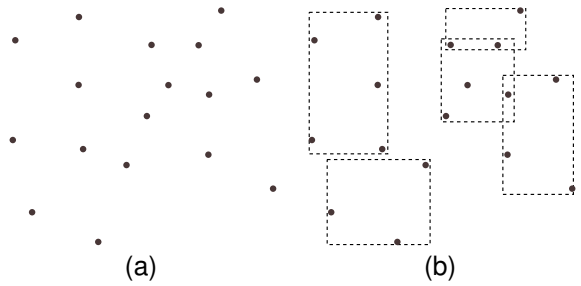

Figure 1: Example of a mapping function Φ_{VERT} in 2D. An initial set of points (a) is mapped to the regions of an overlapping decomposition Δ (b).

4 The Stellar decomposition

The *Stellar decomposition* is a model for data structures representing *Canonical Polytope (CP) complexes*. We denote a CP complex as Σ, and its ordered lists of vertices and top CP cells as Σ_V and Σ_T, respectively. We provide a definition of the Stellar decomposition in Section 4.1 and describe its encoding in Section 4.2.

4.1 Definition

Given a CP complex Σ, a *decomposition* Δ of its vertices Σ_V is a collection of subsets of Σ_V such that every vertex $v \in \Sigma_V$ belongs to at least one of these subsets. We will refer to the elements of decomposition Δ as *regions* and we will denote a region as r.

A Stellar decomposition $\mathbb{S}_{\mathbb{D}}$ defines a map from the regions of a decomposition Δ of its vertex set Σ_V to the vertices and top CP cells of a complex Σ. Formally, a Stellar decomposition is defined by three components:

1. a *CP complex* Σ;
2. a *decomposition* Δ whose regions cover the vertices of Σ;
3. a *map* Φ from regions of Δ to entities of Σ.

Thus, a Stellar decomposition is a triple $\mathbb{S}_{\mathbb{D}} = (\Sigma, \Delta, \Phi)$. Since Σ is entirely characterized by its vertices and top CP cells, we define map Φ in terms of the two components: Φ_{VERT} defines the mapping to vertices and Φ_{TOP} defines the mapping to top CP cells.

For the vertices, we have a map from Δ to Σ_V based on an application-dependent *belonging* property. Formally, $\Phi_{VERT} : \Delta \rightarrow \mathscr{P}(\Sigma_V)$ is a map from Δ to the powerset of Σ_V where

$$\forall r \in \Delta, \Phi_{VERT}(r) = \{v \in \Sigma_V : v \textit{ belongs to } r\}$$

While a region r in Δ is associated with a subset of vertices from Σ_V, the above definition does not limit a vertex $v \in \Sigma_V$ to be in a single region. However, we do require that each vertex belongs to at least one region, i.e. we impose the following additional property:

$$\forall v \in \Sigma_V, \exists r \in \Delta | v \in \Phi_{VERT}(r).$$

Figure 1 illustrates an example over a point set in 2D where mapping function Φ_{VERT} associates points with regions of Δ.

The Stellar decomposition gets its name from the properties of its top cell map Φ_{TOP}. For each region r of Δ, $\Phi_{TOP}(r)$ is the set of all top CP cells of Σ_T incident in one or more vertices of $\Phi_{VERT}(r)$. In other words, $\Phi_{TOP}(r)$ is defined by the union of cells in the star of the vertices in $\Phi_{VERT}(r)$. Formally, $\Phi_{TOP} : \Delta \rightarrow \mathscr{P}(\Sigma_T)$ is a function from the regions of Δ to the powerset of Σ_T, where

$$\forall r \in \Delta, \Phi_{TOP}(r) = \{\sigma \in \Sigma_T | \exists v \in R_{k,0}(\sigma) : v \in \Phi_{VERT}(r)\} \quad (1)$$

Figure 2 illustrates mapping Φ_{TOP} for two regions of the decomposition of Figure 1(b) on a triangle mesh defined over its vertices. We note that Φ_{TOP} is based on a topological rather than a spatial property. A top CP cell σ is only mapped to a region r when one (or more) of its vertices is mapped to r under Φ_{VERT}. Specifically, it does not depend on spatial overlap. To characterize this representation, we define the *spanning number* χ_σ of top cells in a Stellar decomposition as the number of regions to which a top CP cell is mapped.

Definition 4.1 *Given Stellar decomposition* $\mathbb{S}_{\mathbb{D}} = (\Sigma, \Delta, \Phi)$*, the* spanning number χ_σ *of a CP cell* $\sigma \in \Sigma_T$ *is the number of regions in* Δ *that map to* σ*. Formally,*

$$\forall \sigma \in \Sigma_T, \ \chi_\sigma = |\{\mathrm{r} \in \Delta | \sigma \in \Phi_{TOP}(\mathrm{r})\}| \quad (2)$$

It is also interesting to consider the *average spanning number* χ as a global characteristic of the efficiency of a Stellar decomposition over a complex measuring the average number of times each top CP cell is represented.

Definition 4.2 *The* average spanning number χ *of a Stellar decomposition* $\mathbb{S}_{\mathbb{D}}$ *is the average number of regions indexing a top CP cell* σ*. Formally,*

$$\chi = (\sum_{\sigma \in \Sigma_T} \chi_\sigma)/|\Sigma_T| = (\sum_{\mathrm{r} \in \Delta} |\Phi_{TOP}(\mathrm{r})|)/|\Sigma_T| \quad (3)$$

4.2 Encoding

In this section, we describe how we represent the two components of a Stellar decomposition, providing a detailed description of the data structures for representing a CP complex (subsection 4.2.1) and a compressed encoding for the regions of the decomposition (subsection 4.2.2). We do not describe how the decomposition Δ is represented, as this is specific to each concrete realization of the Stellar decomposition model.

4.2.1 Indexed representation of the CP complex

We assume that the underlying CP complex is represented as an indexed complex, which encodes the spatial position

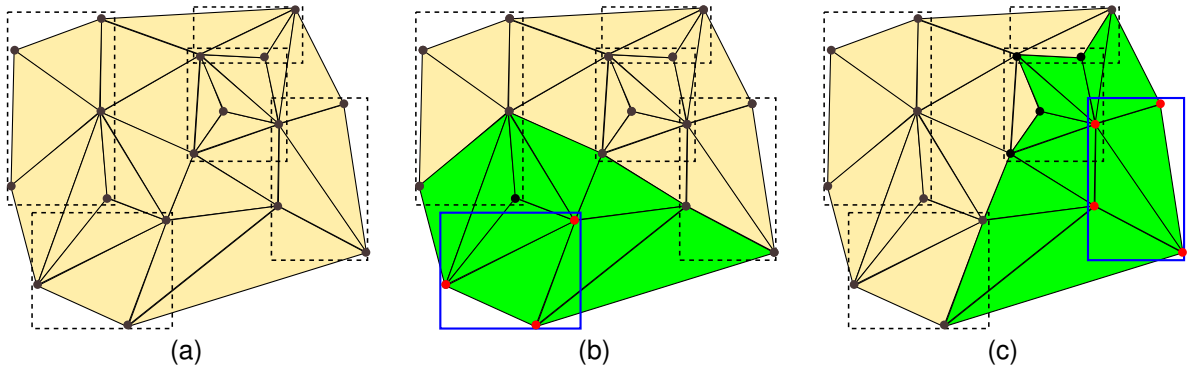

Figure 2: Example mapping function Φ_{TOP} for the decomposition from Figure 1. Given a triangle mesh (a) and a vertex map Φ_{VERT} on decomposition Δ, Φ_{TOP} maps the triangles in the star of the vertices in $\Phi_{VERT}(r)$ to $\Phi_{TOP}(r)$. (b) and (c) highlight the triangles (green) mapped to two different regions (blue) of Δ.

of the vertices and the boundary relation $R_{k,0}$ of each top k-simplex in Σ. In the following, we discuss the case of a d-dimensional CP complex Σ embedded in $\mathbb{E}^n$.

We use an array-based representation for the vertices and top cells of Σ. Since the arrays are stored contiguously, each vertex v has a unique position index i_v in the Σ_V array and similarly each top CP cell σ in the Σ_T array associated with its dimension has a unique position index i_σ. The Σ_V array encodes the position of each vertex v in Σ, requiring a total of $n \cdot |\Sigma_V|$ coordinates. The top CP cells are encoded using separate arrays Σ_{T_k} for each dimension $k \leq d$ that has top CP cells in Σ. Σ_{T_k} encodes the boundary connectivity from its top CP cells to their vertices, i.e., relation $R_{k,0}$ in terms of the indices i_v of the vertices of its cells within Σ_V. This requires $|R_{k,0}(\sigma)|$ references for a top k-cell σ, e.g. (k+1) vertex indices for a k-simplex and 2^k references for a k-cube. Thus, the total storage cost of the indexed mesh representation is:

$$n \cdot |\Sigma_V| + \sum_{k=1}^{d} \sum_{\sigma \in \Sigma_{T_k}} |R_{k,0}(\sigma)|. \tag{4}$$

We note that, in typical cases, where Σ is pure (i.e., its top CP cells all have the same dimension d), Σ requires only two arrays: one for the vertices and one for the top cells.

4.2.2 A compressed region representation

In this subsection, we discuss two encoding strategies for the data mapped to each region of the decomposition. We begin with a simple strategy that explicitly encodes the arrays of vertices and top CP cells mapped to each region and work our way to a compressed representation of these lists. Coupling this compressed representation with a reorganization of the vertices and cells of the CP complex that exploits the spatial locality of its cells (as we will describe in Section 6) yields a significant reduction in storage requirements for a Stellar decomposition, as we will demonstrate in Section 7.2.

Recall that under Φ, each region r in Δ maps to a list of vertices r_V and a list of top CP cells r_T from the complex Σ. A straightforward strategy would be to encode lists of vertices and top CP cells that explicitly list the mapped elements for each region r. We refer to this as the EXPLICIT Stellar decomposition encoding. An example of the EXPLICIT encoding for a single region with six vertices in r_V and twenty triangles in r_T is shown in Figure 3.

It is apparent that the above encoding can be very expensive due to the redundant encoding of top CP cells with vertices in multiple regions. A less obvious redundancy is that it does not account for the locality of the elements induced by the spatial clustering.

We now consider a COMPRESSED Stellar decomposition encoding that compacts the vertex and top CP cells lists in each region r by exploiting the *locality* of

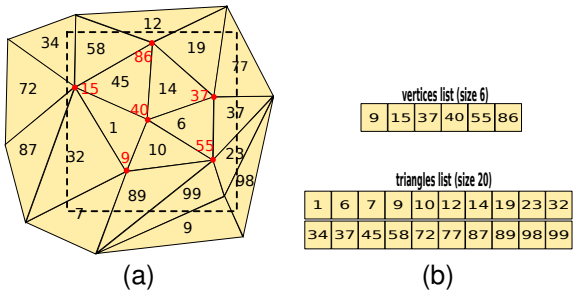

Figure 3: EXPLICIT encoding for triangles within a region (dotted square). The lists explicitly encode the 6 vertices and 20 triangles in the region.

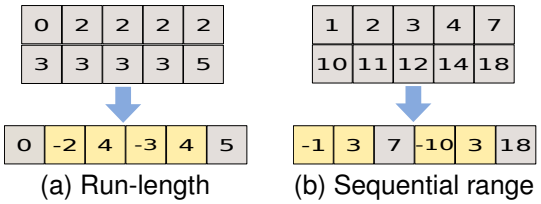

Figure 4: *Run-length* and *sequential range* encodings for sequences of non-negative integers. Runs (a) and sequences (b) are highlighted in yellow.

the elements within r. The COMPRESSED encoding reduces the storage requirements within region lists by replacing *runs* of incrementing consecutive sequences of indices using a generalization of *run-length encoding (RLE)* [Held and Marshall, 1991]. RLE is a form of data compression in which *runs* of consecutive identical values are encoded as pairs of integers representing the value and repetition count, rather than as multiple copies of the original value. For example, in Figure 4a, the four entries with value '2' are compacted into a pair of entries $[-2,4]$, where a negative first number indicates the start of a run and its value, while the second number indicates the run's length.

While we do not have such duplicated runs in our indexed representation, we often have incrementing sequences of indexes, such as $\{40,41,42,43,44\}$, within a local vertex list r_V or top CP cells list r_T. We therefore use a generalized RLE scheme to compress such sequences, which we refer to as *Sequential Range Encoding (SRE)*. SRE encodes a run of *consecutive* non-negative indexes using a pair of integers, representing the starting index, and the number of remaining elements in the range. As with RLE, we can intersperse runs (sequences) with non-runs in the same list by negating the starting index of a run (e.g. $[-40,4]$ for the above example). Thus, it is easy to determine whether or not we are in a run while we iterate through a sequential range encoded list. A nice feature of this scheme is that it allows us to dynamically append individual elements or runs to an SRE list with no storage overhead. Furthermore, we can easily *expand* a compacted range by replacing its entries with the first two values of the range and appending the remaining values to the end of the list. Figure 4b shows an example SRE list over a given sequence, where, e.g., the sequence $\{1,2,3,4\}$ is represented with the pair $[-1,3]$.

In order to compare the EXPLICIT and COMPRESSED representations of the Stellar decomposition, we introduce a global characteristic that measures the average storage requirements for a top CP cell in a Stellar decomposition representation.

Definition 4.3 *The* average reference number μ *of a Stellar decomposition is the average number of references required to encode a top CP cell in the r_T lists of the regions in Δ. Formally:*

$$\mu = (\sum_{r \in \Delta} |r_T|)/|\Sigma_T| \tag{5}$$

where $|r_T|$ is the size of the top CP cells list in a region r.

In contrast to the average spanning number χ, which is a property of the decomposition, the average reference number μ is a property of how the decomposition in encoded. An EXPLICIT representation is equivalent to a COMPRESSED representation without any compressed runs, and, thus, it is always the case that $\mu \leq \chi$. In the EXPLICIT representation (i.e. without any sequence-based compression), $\mu = \chi$, while in the COMPRESSED representation, μ decreases as the compression of the r_T lists becomes more effective. Figure 5 illustrates a COMPRESSED representation of the mesh from Figure 3 after its vertex and triangle arrays have been reordered (in an external process) and highlights its sequential ranges, where r_V requires a single run to encode the indexed vertices and r_T requires four sequential runs to encode the indices of its triangles.

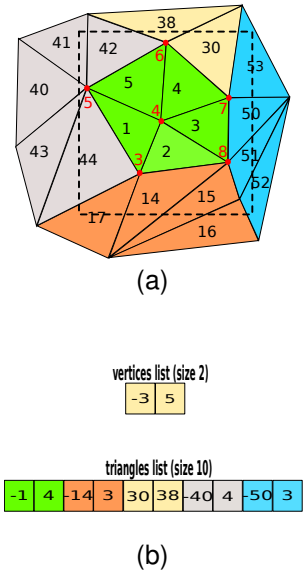

Figure 5: COMPRESSED encoding for triangles within a region (dotted square) after reindexing the vertices and triangles of the mesh from Figure 3.

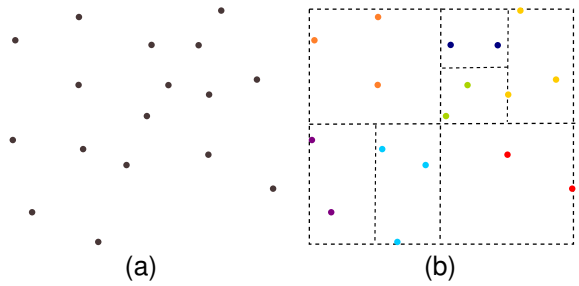

Figure 6: A mapping function Φ_{VERT} over a nested spatial decomposition Δ. An initial set of points (a) is partitioned by the leaf blocks of Δ (b).

5 The Stellar tree

The Stellar decomposition is a general model that is agnostic about how the decomposition is attained and about its relationship to the underlying CP complex. Thus, for example, we can define a Stellar decomposition using Voronoi decompositions or regular or irregular tilings covering the vertices of a given CP complex. In this section, we introduce the *Stellar tree* as a class of Stellar decompositions defined over nested spatial decompositions of the ambient space and discuss some of our design decisions. Before defining a Stellar tree (Section 5.1) and its encoding (Section 5.2), we review some underlying notions.

Background The *ambient space* $\mathbb{A}$ is the subset of $\mathbb{E}^n$ in which the data is embedded. We consider the region bounding the ambient space to be a hyper-rectangular *axis-aligned bounding block*, which we refer to simply as a *block*. A k-dimensional *closed* block b in $\mathbb{E}^n$, with $k \leq n$, is the Cartesian product of k closed intervals $[l_i, u_i]$, with $i = 1, \ldots n$, where exactly k of them are non-degenerate, i.e., $b = \{(x_1, \ldots, x_n) \in \mathbb{E}^n \mid x_i \in [l_i, u_i]\}$ and $\#\{i \mid l_i < u_i\} = k$.

Given two blocks $b := [l_i, u_i]$ and $b' := [l'_i, u'_i]$, b' is a *face* of b if, for each dimension i, either their intervals overlap (i.e. $l'_i = l_i$ and $u'_i = u_i$) or the i^{th} interval of b' is degenerate (i.e. $l'_i = u'_i = l_i$, or $l'_i = u'_i = u_i$). Moreover, b' is a *proper face* of b if $b' \neq b$. Given a block b, we refer to its 0-dimensional face of degenerate intervals $x_i = l_i$ as its *lower corner* and to its 0-dimensional face where $x_i = u_i$ as its *upper corner*.

The above block definition describes *closed* blocks. It can be useful to allow some faces of b to be *open*, especially on faces of neighboring blocks that overlap only on their boundaries. A k-dimensional *half-open* block b in $\mathbb{E}^n$ is defined as $b = \{(x_1, \ldots, x_n) \in \mathbb{E}^n \mid x_i \in [l_i, u_i)\}$ and $\#\{i \mid l_i < u_i\} = k$. Note that all faces of a half-open block b incident in its lower corner are *closed*, while all other faces of b are *open*.

We now focus on *nested decompositions*, hierarchical space-based decompositions whose overlapping blocks are nested and whose leaf blocks Δ_L (i.e. those without any nested blocks) form a non-overlapping cover of the ambient space $\mathbb{A}$. The nesting relationship of the blocks defines a *containment hierarchy* $\mathbb{H}$, which can be described using a rooted *tree*. The root $\mathbb{H}_{ROOT}$ of the tree covers the ambient space $\mathbb{A}$; the leaves $\mathbb{H}_L$ of the tree correspond to the set of leaf blocks Δ_L of the decomposition; and the internal nodes $\mathbb{H}_I$ of the tree correspond to the internal blocks Δ_I of the decomposition.

Nested decompositions can adopt different hierarchical refinement strategies. Among the most popular are those based on *regular* refinement and *bisection* refinement of simple primitives (e.g. simplices and cubes). A n-dimensional block b is regularly refined by adding vertices

at all edge and face midpoints of b and replacing b with 2^n disjoint blocks covering b. This generates *quadtrees* in 2D, and *octrees* in 3D [Samet, 2006]. In bisection refinement, a block is bisected along an axis-aligned hyperplane into two blocks, generating *kD-trees* [Bentley, 1975].

5.1 Definition

Since a Stellar tree $\mathbb{S}_\mathbb{T}$ is a type of Stellar decomposition, it consists of three components: 1. a *CP complex* Σ embedded in an *ambient space* $\mathbb{A}$; 2. a *nested decomposition* Δ covering the domain of Σ; and 3. a *map* Φ from blocks of Δ to entities of Σ. The nested decomposition is described by a containment hierarchy $\mathbb{H}$, represented by a *tree* whose blocks use the *half-open* boundary convention to ensure that every point in the domain is covered by exactly one leaf block.

Since Stellar trees are defined over nested spatial decompositions that cover the ambient space, we customize the vertex mapping function Φ_{VERT} to partition the vertices according to spatial containment: each vertex is mapped to its single containing leaf block. Formally,

$$\forall b \in \Delta_L, \Phi_{VERT}(b) = \{v \in \Sigma_V : v \cap b \neq \emptyset\} \qquad (6)$$

A 2D example is shown in Figure 6, where a set of points are mapped to the leaf blocks of Δ through Φ_{VERT}.

The top CP cells mapping function Φ_{TOP} for a Stellar tree has the same definition as for the Stellar decomposition (see Equation 1). However, a consequence of the unique mapping of each vertex in Φ_{VERT} is that it provides an upper bound on the spanning number of a cell in a Stellar tree. Specifically, the spanning number χ_σ of a CP cell σ is bounded by the cardinality of its vertex incidence relation $R_{k,0}$: $1 \leq \chi_\sigma \leq |R_{k,0}(\sigma)|$. Figure 7 shows the mapping Φ_{TOP} for two blocks of the nested kD-tree decomposition of Figure 6(b) over the triangle mesh from Figure 2.

Once we have defined all the components that form a Stellar tree, we must decide how to generate efficient decompositions of the ambient space in which Σ is embedded. Since the nested decomposition Δ, and consequently the tree $\mathbb{H}$ describing it, are determined by the number of vertices indexed by a block, we utilize a *bucket PR tree* to drive our decomposition. This provides a single tuning parameter, the *bucketing threshold*, which we denote as k_V, that uniquely determines the decomposition for a given complex Σ. Recall that a block b in a bucket PR-tree is considered *full* when it indexes more than k_V vertices (in our case, when $|\Phi_{VERT}(b)| > k_V$). Insertion of a vertex into a full block causes the block to refine and to redistribute its indexed vertices among its children.

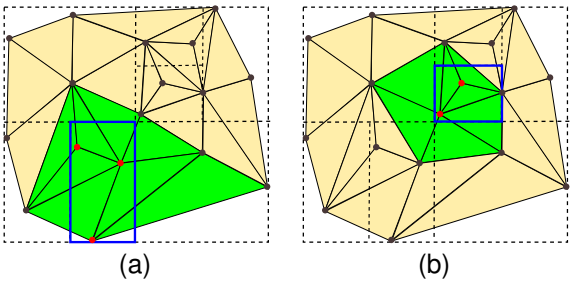

Figure 7: Top cell mapping function Φ_{TOP} for two blocks (highlighted in blue) of the nested decomposition from Figure 6 on the triangle mesh from Figure 2. $\Phi_{TOP}(b)$ maps the triangles in the star of the vertices in $\Phi_{VERT}(b)$.

As such, the domain decomposition of a Stellar tree depends only on the bucketing threshold k_V. Smaller values of k_V yield deeper hierarchies whose leaf blocks index relatively few vertices and top CP cells, while larger values of k_V yield shallower hierarchies with leaf blocks that index more vertices and top CP cells. In other words, k_V and the average spanning number χ of a Stellar tree are inversely correlated: χ decreases as k_V increases, and top CP cells are, on average, indexed by fewer leaf blocks.

5.2 Encoding

We represent the containment hierarchy $\mathbb{H}$ using an *explicit pointer-based* data structure, in which the blocks of $\mathbb{H}$ use a type of `Node` structure that changes state from leaf to internal block during the generation process of a Stellar tree (described in detail in Section 6).

We use a *brood-based* encoding [Hunter and Willis, 1991] where each block in $\mathbb{H}$ encodes a pointer to its parent block and a single pointer to its brood of children. This reduces the overall storage since leaves do not need to encode pointers to each child, and also allows us to use the same representation for n-dimensional quadtrees and kD-trees. We explicitly encode all internal blocks, but only represent leaf blocks b in $\mathbb{H}$ with non-empty maps $\Phi(b)$.

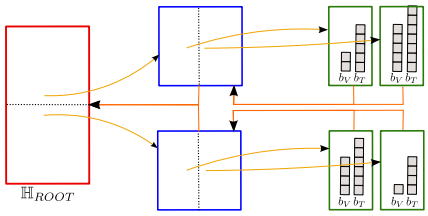

Figure 8: A Stellar tree hierarchy $\mathbb{H}$ over a pure complex. The *red* and *blue* rectangles identify the internal blocks $\mathbb{H}_I$ while the *green* ones represent the leaf blocks $\mathbb{H}_L$ along with their collections of vertices and top CP cells.

The mapped entities of the CP complex Σ are encoded in the leaf blocks $\mathbb{H}_L$ using the mapping function lists:

1. a list b_V of vertex indices in Σ_V defined by $\Phi_{VERT}(b)$;
2. a list of lists b_T of top CP cell indices in Σ_T defined by $\Phi_{TOP}(b)$.

Note that each leaf block b encodes the lists of vertices b_V and of top CP cells b_T in terms of the indices i_v and i_σ, respectively, that identify v and σ in the Σ_V and Σ_T arrays.

Thus, the hierarchy $\mathbb{H}$ of a Stellar tree requires $7|\mathbb{H}|$ storage. For each block b we have:

1. three pointers for the hierarchy: one pointer to its parent, another to its list of children and it is pointed to by one parent;
2. a pointer to a list of vertices b_V and the size of this list;
3. a pointer to a list of top CP cells b_T and the size of this list.

Figure 8 illustrates a simple containment hierarchy representation.

Considering the encodings defined in Section 4.2.2, we can estimate the storage requirements for the EXPLICIT and COMPRESSED Stellar trees. The EXPLICIT Stellar tree requires a total of $|\Sigma_V|$ references for all such vertex lists, since each vertex is indexed by a single leaf block, and a total of $\chi \cdot |\Sigma_T|$ references for all top CP cells lists. Thus, the total cost of the EXPLICIT Stellar tree, including the hierarchy (excluding the cost of the indexed mesh) is:

$$7|\mathbb{H}| + |\Sigma_V| + \chi|\Sigma_T|. \tag{7}$$

Conversely, in a COMPRESSED Stellar tree, we can reindex the vertex array Σ_V such that all vertices mapped to the same leaf block are indexed consecutively (see Section 6.1). Thus, we can encode the b_V lists using only two integers per leaf block for a total cost of $2 \cdot |\mathbb{H}_L|$ rather than $|\Sigma_V|$. Moreover, since leaf blocks no longer need to reference an arbitrary list, these two references can be folded into the block's hierarchical representation for b_V (i.e. instead of a pointer to a list and a size of the list, we simply encode the range of vertices in the same space). As the cost of representing the b_T lists is $\mu \cdot |\Sigma_T|$, the total cost for encoding a COMPRESSED Stellar tree (excluding the cost of the indexed mesh representation) is:

$$7|\mathbb{H}| + \mu|\Sigma_T|. \tag{8}$$

6 Generating a Stellar tree

In this section, we describe how to generate a COMPRESSED Stellar tree from an indexed CP complex Σ in arbitrary dimensions. This process is organized into four main phases:

1. generate the nested decomposition $\mathbb{H}$ by inserting the vertices Σ_V into a bucket PR tree with a given bucket threshold k_V;
2. reindex the vertices of Σ according to a traversal of the leaf blocks of $\mathbb{H}$ and compress the b_V arrays using SRE;
3. insert the top CP cells of Σ into $\mathbb{H}$;
4. reindex the top CP cells of Σ based on locality within common blocks of $\mathbb{H}$ and compress the b_T arrays using SRE.

Our first step is to generate the tree hierarchy $\mathbb{H}$ over the vertices of the complex Σ. Given a user-defined bucket threshold k_V, we utilize a bucket PR tree index over the vertices Σ_V to generate a Stellar nD quadtree or kD-tree decomposition. This is the only phase of our generation process that depends on the geometry of Σ. Although we do not maintain the spatial extents of each tree block, we can reconstruct them from that of the hierarchy's root $\mathbb{H}_{ROOT}$ (based on a bounding box enclosing Σ) by tracking the split planes as we descend the tree.

The procedure for inserting a vertex v with index i_v in Σ_V into $\mathbb{H}$ is recursive. We use the geometric position of v to traverse through the internal blocks to the unique leaf block b containing v. After adding v to b (i.e., appending

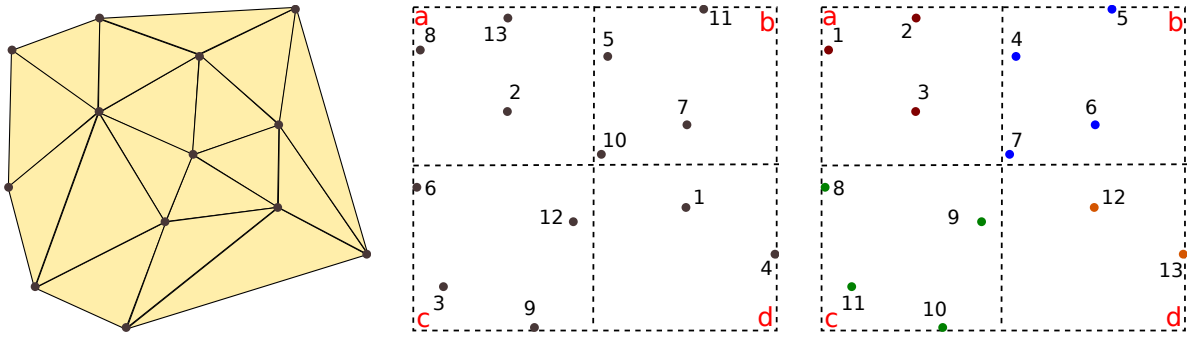

(a) Base mesh $\Sigma := (\Sigma_V, \Sigma_T)$ (b) Vertices inserted ($k_V = 4$) (c) Reindexed vertices

Figure 9: Generating a nested hierarchy $\mathbb{H}$ over the vertices Σ_V of a triangle mesh (a). After inserting the vertices (b), we reindex Σ_V according to $\mathbb{H}_L$ (c).

Algorithm 1 COMPRESS_AND_REINDEX_VERTICES

Require: $\mathbb{H}_{ROOT}$ is the root block of $\mathbb{H}$
Require: Σ is the CP complex
1: $v\_permutation$.INIT($|\Sigma_V|, 0$)
// Step 1: Generate and apply new block vertex index ranges //
2: COMPRESS_TREE_VERTS($\mathbb{H}_{ROOT}, 0, v\_permutation$)
// Step 2: Update the vertex boundary relation //
3: **for all** top simplices σ in Σ_T **do**
4: **for** $j = 0$ to $|R_{k,0}(\sigma)|$ **do**
5: $R_{k,0}(\sigma)[j] \leftarrow v\_permutation[R_{k,0}(\sigma)[j]]$
// Step 3: Update the vertex array indices //
6: UPDATE_ARRAY($\Sigma_V, v\_permutation$)

Algorithm 2 COMPRESS_TREE_VERTS

Require: b is a block in $\mathbb{H}$
Require: *counter* refers to the current vertex id
Ensure: $v\_permutation$ array contains new vertex indices
1: $b.v\_start = counter$
2: **if** $b \in \mathbb{H}_I$ **then**
3: **for all** blocks c in CHILD(b) **do**
4: COMPRESS_TREE_VERTS($c, counter, v\_permutation$)
5: **else** // b $\in \mathbb{H}_L$ //
6: **for all** vertices v in $\Phi_{VERT}(b)$ (with index i_v in Σ_V) **do**
7: $v\_permutation[i_v] \leftarrow counter{+}{+}$
8: $b.v\_end = counter$

i_v into the b_V array of b), we check if the current block overflows the bucketing threshold k_V. If it does, we refine b, reinsert its indexed vertices into its children, and, clear b_V. Once the vertices are inserted, the decomposition is fixed. We then reindex the vertices following a traversal of the leaf blocks of $\mathbb{H}$ such that all vertices mapped to a leaf block have a contiguous range of indices in the reindexed Σ_V (as detailed in Section 6.1). Figure 9 illustrates a reindexing of the vertices of a planar triangle mesh in the plane while generating a decomposition with $k_V = 4$.

After generating the nested decomposition and reindexing the mesh vertices, we insert each top CP k-cell σ of Σ_{T_k}, with index i_σ in Σ_{T_k} into the leaf blocks of $\mathbb{H}$ that index its vertices. That is, we iterate through $R_{k,0}(\sigma)$ and insert i_σ into the b_T list of each block b whose vertex map $\Phi_{VERT}(b)$ contains at least one of these vertices. As such, each top CP k-cell σ appears in at least one leaf block of $\mathbb{H}$, and in at most $R_{k,0}(\sigma)$ leaf blocks of $\mathbb{H}$. Due to the vertex reindexing of step (2), this operation is extremely efficient. Determining if a cell's vertex lies in a block requires only a range comparison on its index i_v, rather than a geometric *point-in-box* test against its position.

Finally, we reindex the top CP cell arrays Σ_T to better exploit the locality induced by the vertex-based decomposition and compress the local b_T arrays using a sequential range encoding over this new index. The reindexing and the compression of the top CP cells is obtained following some traversal of the leaf blocks of $\mathbb{H}$, such that, all top CP cells mapped by the same set of leaf blocks have a contiguous range of indices in the reindexed Σ_T. This last step

Algorithm 3 COMPRESS_AND_REINDEX_CELLS

Require: $\mathbb{H}_{ROOT}$ is the root block in $\mathbb{H}$
Require: Σ is the CP complex
Require: I is an array associated with the unique leaf tuples in M
Require: $t\_position$ is an array associated with the top CP cells
1: $t\_position$.INIT($|\Sigma_T|, 0$)
// Step 1: find unique leaf block tuples and counts //
2: EXTRACT_LEAF_TUPLES($\mathbb{H}_{ROOT}$,I,t_position)
// Step 2: find new position indices of top CP cells //
3: EXTRACT_CELL_INDICES(I,t_position)
// Step 3: reorder and SRE compact the top CP cells arrays //
4: COMPRESS_TREE_CELLS($\mathbb{H}_{ROOT}$,t_position)
// Step 4: update the top CP cells array in Σ //
5: UPDATE_ARRAY($\Sigma_T, t\_position$)

is detailed in Section 6.2. As we demonstrate in Section 7, this yields a significant storage savings.

6.1 Reindexing and compressing the vertices

After generating the nested decomposition Δ and vertex map Φ_{VERT} for the Stellar tree, we reindex the vertex array Σ_V to better exploit the *spatial coherence* induced by Δ. At the end of this process, each block of $\mathbb{H}$ has a consecutive range of indices within the global vertex array Σ_V. Since each block has a single contiguous range of vertex indices, it trivially compresses under SRE to two values per block, which we denote as v_{start} and v_{end}.

This reindexing procedure is organized into three main steps as outlined in Algorithm 1 and is aided by an auxiliary array `v_permutation` which stores the new index for each vertex in Σ_V.

We first perform a depth first traversal of the tree (see Algorithm 2) which generates new indices for the mesh vertices. For each leaf block b, this provides a contiguous range of indices for the list of mapped vertices b_V, while for internal blocks, this provides a single contiguous index range for the vertices in all descendant blocks. The new index is then incorporated into the mesh Σ by replacing the vertex indices in the vertex-boundary relation arrays (Algorithm 1, Step 2) and in the vertex array (Algorithm 1, Step 3).

6.2 Reindexing and compressing the top CP cells

After inserting the top CP cells of Σ_T into $\mathbb{H}$, we exploit the spatial coherence of the top CP cells array Σ_T and compress the tree representation using the COMPRESSED encoding. This procedure is organized into four main phases (see Algorithm 3):

1. navigate the tree to find, for each top CP cell σ, the tuple of leaf blocks that index it. We invert this relation to find, for each such tuple of leaves, the list of top cells mapped to its leaves;
2. generate a new spatially coherent ordering for the top CP cells of Σ_T based on the inverted relation from the previous step;
3. apply this ordering to the b_T lists of each block and compact the b_T leaf block arrays using SRE compression;
4. update Σ_T using the new spatially coherent ordering.

Algorithm 3 requires three auxiliary data structures:

1. an associative array, `M`, which maps an (integer) identifier to each unique tuple of leaf blocks;
2. an array of integers, `I`, having the same number of entries as `M`. Initially, it is used to track the number of top CP cells associated with each tuple of leaf blocks. In a successive phase, it tracks the next index for a top CP cell in a leaf tuple;
3. an array of integers, `t_position`, of size $|\Sigma_T|$. Initially, it is used to associate top CP cells with their leaf tuple identifier. In a successive phase, it is used to store the new spatially coherent indices for the top CP cells.

Thus, the storage overhead for the auxiliary structures is $|\Sigma_T|$ for the `t_position` and $O(|\mathtt{M}|)$ for the map `M` and the array `I`.

The reindexing exploits the spatial coherence of top CP cells that are contained into the same set of leaves by translating spatial proximity in $\mathbb{A}$ into index-space proximity in Σ_T. Figure 10 illustrates this reorganization process over a simple 2D triangle mesh. In the remainder of this section, we summarize the major steps of Algorithm 3.

In the first step (Algorithm EXTRACT_LEAF_TUPLES), we generate map `M`, count the number of top CP cells associated with each tuple of leaf blocks in array `I` and initialize the `t_position` array entries with its tuple identifier. For each leaf block b in $\mathbb{H}$, we visit the top CP cells σ in

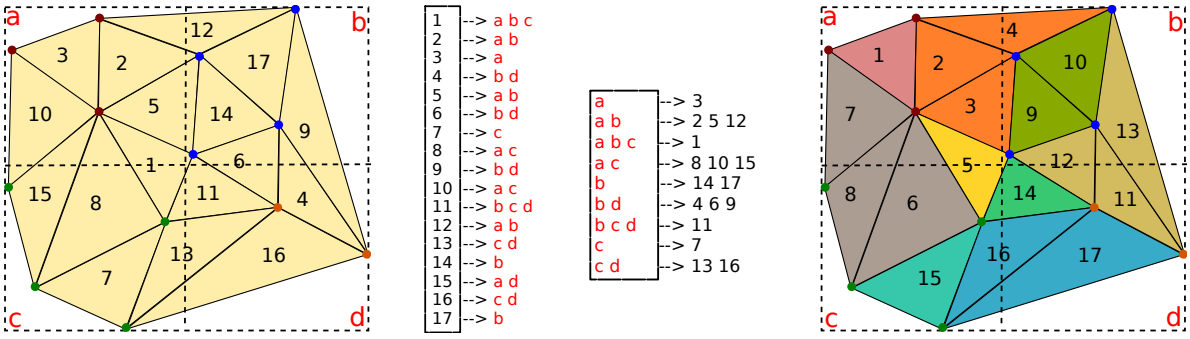

(a) Original tree (b) Triangles and leaves associations (c) Reindexed triangles

Figure 10: Top cell reindexing. (a) initial tree with four leaf blocks a, b, c, d (b) maps between triangles and tuples of leaf blocks (c) reindexed tree.

Φ_{TOP}(b) whose minimum vertex index i_v is indexed in b. This ensures that each top CP cell is only visited a single time. Blocks of $\mathbb{H}$ are uniquely indexed by the index of their starting vertex v_{start}.

For each such top CP cell σ with index i_σ, we traverse the tree to find the tuple of leaf blocks from the tree that index σ. We then look up its unique identifier *key* in `M` (or create a new one and insert it into `M`). We then increment the count for this tuple (`I[`*key*`]++`), and associate σ with this tuple (`t_position[`i_σ`]=`*key*).

Once we have visited $\mathbb{H}$, each entry of `t_position` contains the identifier of the tuple of leaf blocks indexing its corresponding top cell and `I` contains the number of top CP cells indexed by each leaf tuple. `M` is no longer needed and we can discard it.

In the next step (Algorithm EXTRACT_CELL_INDICES), we use the `I` and `t_position` arrays to find the updated position for each top CP cell in Σ_T, which is computed in place in `t_position`. First, we convert the cell counts in array `I` into starting indexes for the top CP cells grouped by the same set of leaf blocks by taking the prefix sum of array `I` (`I=prefixSum(I)`). We then use array `I` to update the `t_position` array by looping through the top CP cells, and replacing the tuple identifier in `t_position` with the next available index from `I` and increment the counter in `I` (`t_position[`i_σ`] = I[t_position[`i_σ`]]++`). At this point, `t_position` is a permutation array that encodes a more spatially coherent ordering for the top CP cells and `I` is no longer needed.

Finally (Algorithm COMPRESS_TREE_CELLS), we apply the new ordering from array `t_position` to the local b_T arrays and sort and SRE compress them. We then use `t_position` to permute the global top CP cells array Σ_T.

7 Evaluation of storage costs

In this section, we evaluate the storage costs of the indexed representation for the underlying CP complex and compare the Stellar tree to several state-of-the-art topological mesh data structures. After introducing the datasets used in our experimental evaluation (Section 7.1), we compare the cost of different Stellar tree encodings (Section 7.2). We then compare the Stellar tree against state-of-the-art topological data structures (Section 7.3).

7.1 Experimental datasets

We have performed experiments on a range of CP complex datasets consisting of triangle, quadrilateral, tetrahedral and hexahedral meshes in $\mathbb{E}^3$ as well as several pure non-manifold higher dimensional simplicial complexes generated through a recursive Sierpinski-like refinement process and several higher dimensional simplicial complexes generated through a Vietoris-Rips generation tool (using

Data		$\lvert\Sigma_V\rvert$	$\lvert\Sigma_T\rvert$		k_V	$\lvert\mathbb{H}\rvert$	$\lvert\mathbb{H}_L\rvert$	χ
NEPTUNE	TRIANGULAR	2.00M	4.01M	k_S	100	73.7K	58.8K	1.37
				k_L	500	15.0K	12.2K	1.17
STATUETTE		5.00M	10.0M	k_S	100	182K	147K	1.36
				k_L	500	39.8K	32.7K	1.17
LUCY		14.0M	28.1M	k_S	100	464K	374K	1.35
				k_L	500	88.8K	70.3K	1.16
NEPTUNE	QUAD	12.0M	12.0M	k_S	100	407K	322K	1.47
				k_L	800	55.0K	44.3K	1.17
STATUETTE		30.0M	30.0M	k_S	100	1.10M	883K	1.47
				k_L	800	146K	120K	1.17
LUCY		84.1M	84.2M	k_S	100	3.53M	2.85M	1.54
				k_L	800	329K	265K	1.17
BONSAI	TETRAHEDRAL	4.25M	24.4M	k_S	400	45.2K	39.5K	1.58
				k_L	800	17.9K	15.7K	1.44
VISMALE		4.65M	26.5M	k_S	400	32.8K	28.7K	1.52
				k_L	800	17.7K	15.5K	1.45
FOOT		5.02M	29.5M	k_S	400	88.8K	77.7K	1.75
				k_L	800	17.1K	15.0K	1.43
F16	HEXAHEDRAL	27.9M	25.4M	k_S	100	1.11M	972K	3.08
				k_L	1000	113K	99.0K	1.90
SAN FERN		61.3M	55.9M	k_S	100	2.02M	1.77M	3.15
				k_L	1000	247K	216K	1.88
VISMALE		136M	125M	k_S	100	7.39M	6.46M	2.8
				k_L	1000	800K	700K	1.72
5D	PROBABILISTIC	383K	26.5M	k_S	100	37.4K	36.1K	4.39
				k_L	500	2.79K	2.68K	2.55
7D		239K	258M	k_S	100	10.8K	4.87K	4.98
				k_L	500	2.02K	1.00K	3.78
40D		204K	16.5M	k_S	100	15.2K	4.32K	36.2
				k_L	1000	1.56K	550	34.0
VISMALE 7D	V-RIPS	4.65M	6.39M	k_S	400	32.8K	28.7K	1.44
				k_L	800	17.7K	15.5K	1.37
FOOT 10D		5.02M	63.9M	k_S	400	88.8K	77.7K	2.02
				k_L	800	17.1K	15.0K	1.56
LUCY 34D		14.0M	41.1M	k_S	100	464K	374K	2.47
				k_L	500	88.8K	70.3K	1.73

Table 1: Overview of experimental datasets and the generated Stellar trees. For each dataset, we list the type of CP complex and the number of vertices $\lvert\Sigma_V\rvert$ and top CP cells $\lvert\Sigma_T\rvert$. For each Stellar tree, we list the thresholds k_V, the number of blocks in the index (total $\lvert\mathbb{H}\rvert$ and leaf $\lvert\mathbb{H}_L\rvert$) and the average spanning number χ.

the algorithm from [Zomorodian, 2010]) and embedded in $\mathbb{E}^3$.

The triangle and tetrahedral meshes are *native* models ranging from 4 to 28 million triangles and from 24 to 29 million tetrahedra, where we use the term native to refer to models from public domain repositories discretizing objects in space. Since we only had access to relatively small native quad and hex meshes (with tens to hundreds of thousand elements), we have generated some larger models ranging from 12 to 125 million elements from our triangle and tetrahedral models. The generation procedure refines each triangle into three quadrilaterals and each tetrahedron into four hexahedra by adding vertices at the face centroids.

To experiment with *pure* non-manifold models in higher dimensions, we have generated some models based on a process that we call *probabilistic Sierpinski filtering*, where we iteratively apply regular refinement to all simplices in the complex and randomly remove a fixed proportion of the generated simplices in each iteration. For our experiments, we have created 5-, 7- and 40-dimensional models using a filtering threshold of 65%, with differing levels of refinement, yielding pure simplicial complexes with 16.5 million to 258 million top simplices.

Finally, to experiment with general simplicial complexes in higher dimensions, we have generated several (non-pure) non-manifold higher dimensional *Vietoris-Rips (V-Rips)* complexes, which we embed in a lower dimensional space. A V-Rips complex is a *flag* complex defined by a neighborhood graph over a point cloud whose arcs connect pairs of points with distance less than a user-provided parameter ε. Given the neighborhood graph, the simplices of the V-Rips complexes are defined by its *cliques*, subsets of the graph vertices that form a complete subgraph. We refer to [Zomorodian, 2010] for further details. For our experiments, we have generated three V-Rips models over the vertices of a triangle model (LUCY) and of two tetrahedral models (VISMALE and FOOT) from our manifold datasets and set our distance threshold ε to $\{0.1\%, 0.5\%, 0.4\%\}$ of the bounding box diagonal, respectively. The generated complexes range from 6.39 million to 63.9 million top simplices and from dimensions 7 to 34. Although the generated datasets are synthetic, they provide a good starting point to demonstrate the efficiency of the Stellar tree in higher dimensions.

For every model, we have built two Stellar trees to com-

pare the dependence of the performance on our single parameter k_V, which determines the maximum number of vertices that each leaf block of the tree can index. These two k_V values are chosen to obtain trees with different characteristics: one extremely deep and the other relatively coarse. We have also attempted to maintain similar χ values across the datasets. In the following, we use k_S to refer to the smaller k_V value and k_L for the larger one.

We have also used different spatial indexes to represent the containment hierarchy $\mathbb{H}$ based on the dimension n of the ambient space $\mathbb{A}$: in *low* dimensions, we use a quadtree-like subdivision, and thus, we have a quadtree in 2D, an octree in 3D, and so on, up to 6D; in dimensions *higher* than 6, we switch to a kD-tree subdivision. While quadtree-like subdivisions are quite efficient in lower dimension, the data becomes sparser in higher dimensions and is better modeled by kD-trees with fewer spatial splits [Samet, 2006].

Table 7.1 summarizes the number of elements and the sizes of the spatial decompositions for the two Stellar tree representations (k_S and k_L) of each experimental dataset. All tests have been performed on a PC equipped with a 3.2 gigahertz Intel i7-3930K CPU with 64 gigabytes of RAM.

7.2 Analysis of Stellar tree encodings

We begin by comparing the EXPLICIT and COMPRESSED Stellar tree encodings as well as a VERTEX-COMPRESSED encoding, similar to the PR-star encoding for tetrahedral meshes [Weiss et al., 2011] that compresses only the vertices array but not the top cells arrays. Table 7.2 lists the storage costs for the indexed 'Base Mesh' as well as the additional costs required for the three Stellar tree encodings, in terms of megabytes (*MBs*). Note that Stellar trees based on the COMPRESSED encoding are always the most compact.

We first consider the storage requirements of the hierarchical structures and observe that higher values of k_V yield significant reductions in memory requirements for the COMPRESSED representation. Whereas the EXPLICIT and VERTEX-COMPRESSED k_L representations only obtain about a 20-50% reduction in storage requirements compared to their k_S counterparts (e.g. 26.2 MB vs. 32.0 MB for the EXPLICIT NEPTUNE dataset), the COMPRESSED k_L datasets are 3-10 times as compact as their k_S counterparts (e.g. 1.24 MB vs. 5.76 MB for the COMPRESSED

Data			Base mesh	Stellar tree					
				EXPLICIT		VERTEX		COMPRESS	
				cost	χ	cost	χ	cost	μ
NEPTUNE	TRIANGULAR	k_S	45.9	32.0	1.37	24.3	1.37	5.76	0.16
		k_L		26.2	1.17	18.6	1.17	1.24	0.04
STATUETTE		k_S	114	79.2	1.36	60.2	1.36	14.6	0.17
		k_L		65.6	1.17	46.6	1.17	3.41	0.04
LUCY		k_S	321	220	1.35	166	1.35	34.5	0.12
		k_L		181	1.16	128	1.16	6.18	0.02
NEPTUNE	QUAD	k_S	183	132	1.47	86.0	1.47	28.0	0.20
		k_L		102	1.17	56.3	1.17	3.86	0.03
STATUETTE		k_S	458	333	1.47	219	1.47	76.0	0.22
		k_L		255	1.17	141	1.17	10.4	0.03
LUCY		k_S	1.3K	976	1.54	656	1.54	245	0.26
		k_L		710	1.17	389	1.17	23.1	0.03
BONSAI	TETRAHEDRAL	k_S	373	166	1.58	150	1.58	6.55	0.05
		k_L		151	1.44	135	1.44	2.65	0.02
VISMALE		k_S	405	173	1.52	156	1.52	4.87	0.03
		k_L		165	1.45	147	1.45	2.69	0.02
FOOT		k_S	450	220	1.75	201	1.75	13.0	0.08
		k_L		181	1.43	161	1.43	2.60	0.02
F16	HEXAHEDRAL	k_S	775	456	3.08	349	3.08	151	1.03
		k_L		296	1.90	189	1.90	18.0	0.13
SAN FERN		k_S	1.7K	999	3.15	765	3.15	275	0.86
		k_L		646	1.88	412	1.88	33.1	0.10
VISMALE		k_S	3.8K	2.2K	2.89	1.7K	2.89	887	1.15
		k_L		1.4K	1.72	858	1.72	106	0.15
5D	PROBABILISTIC	k_S	607	448	4.39	446	4.39	63.7	0.61
		k_L		259	2.55	258	2.55	3.57	0.03
7D		k_S	7.9K	4.9K	4.98	4.9K	4.98	101	0.10
		k_L		3.7K	3.78	3.7K	3.78	12.2	0.01
40D		k_S	2.6K	2.3K	36.2	2.3K	36.2	55.7	0.87
		k_L		2.1K	34.0	2.1K	34.0	0.45	0.01
VISMALE 7D	V-RIPS	k_S	134	56.2	1.44	37.0	1.44	7.38	0.26
		k_L		53.7	1.37	34.6	1.37	4.54	0.18
FOOT 10D		k_S	2.1K	604	2.02	586	2.02	65.1	0.33
		k_L		431	1.56	413	1.56	11.5	0.12
LUCY 34D		k_S	2.0K	416	2.47	363	2.47	86.2	0.92
		k_L		292	1.73	238	1.73	19.0	0.53

Table 2: Storage costs (in *MB*s) and average spanning (χ) and reference (μ) numbers for different Stellar tree encodings.

NEPTUNE dataset).

Next, comparing the three encodings, we see that SRE compressing the vertices alone, as in the VERTEX-COMPRESSED representation achieves only 10-20% reduction in storage requirements compared to the EXPLICIT representation. In contrast, compressing the vertices and top cells, as in our COMPRESSED representation, yields an order of magnitude improvement, requiring around 10-20 times less storage. This trend is nicely tracked by comparing the average references number μ to the average spanning number χ, where χ is typically around ten times larger than μ.

Considering the hierarchical storage requirements against those of the original indexed base mesh, we observe that EXPLICIT Stellar trees require about 50% to 80% the storage of the base mesh, while COMPRESSED Stellar trees require only about around 10% (k_S) and 1% (k_L) the storage of the EXPLICIT representation. Thus, practically the entire storage costs for the COMPRESSED representation are due to the underlying indexed mesh.

In the remainder of this paper, we restrict our attention to the COMPRESSED Stellar Tree, which we will refer to simply as *the* Stellar tree.

7.3 Comparison with dimension-independent data structures

In this subsection, we compare the Stellar tree to the topological data structures proposed in the literature for simplicial complexes.

Based on our analysis of the literature (see Section 3.1), the most relevant dimension-independent topological data structures to the Stellar tree are: the Incidence Graph (IG), the Incidence Simplicial (IS), the Simplex tree and the IA* data structures. Since Canino et al. demonstrated that the IA* data structure is more compact than the IG and the IS data structures for low and higher-dimensional datasets [Canino et al., 2011, Canino and De Floriani, 2014], we restrict our comparisons to the IA* data structure and the Simplex tree.

The IA* data structure has been defined for dimension-independent simplicial complexes, and in this work it has been extended to dimension-independent CP complexes. It explicitly encodes all vertices and top CP k-cells in Σ, with $0 < k \leq d$, as well as the following relations:

(i) boundary relation $R_{k,0}(\sigma)$ for each top CP k-cell σ;

Data		k_V	Storage					
			mesh	IA*		Simplex	Stellar tree	
				conn.	tot	tree	index	tot
NEPTUNE	TRIANGULAR	k_S	45.9	53.5	99.4	321	5.76	51.6
		k_L					1.24	47.1
STATUETTE		k_S	114	134	248	801	14.6	129
		k_L					3.41	118
LUCY		k_S	321	374	695	2.2K	34.5	355
		k_L					6.18	327
NEPTUNE	QUAD	k_S	183	229	413	n.a.	28.0	211
		k_L					3.86	187
STATUETTE		k_S	458	572	1.0K	n.a.	76.0	534
		k_L					10.4	468
LUCY		k_S	1.3K	1.6K	2.9K	n.a.	245	1.5K
		k_L					23.1	1.3K
BONSAI	TETRAHEDRAL	k_S	373	389	762	2.8K	6.55	379
		k_L					2.65	375
VISMALE		k_S	405	470	875	3.1K	4.87	410
		k_L					2.69	408
FOOT		k_S	450	470	920	3.4K	13.0	463
		k_L					2.60	453
F16	HEXAHEDRAL	k_S	775	688	1.5K	n.a.	151	926
		k_L					18.0	793
SAN FERN		k_S	1.7K	1.5K	3.2K	n.a.	275	2.0K
		k_L					33.1	1.7K
VISMALE		k_S	3.8K	3.4K	7.2K	n.a.	887	4.7K
		k_L					106	3.9K
5D	PROBABILISTIC	k_S	607	608	1.2K	7.1K	63.7	670
		k_L					3.57	610
7D		k_S	7.9K	7.9K	15.8K	155K	101	8.0K
		k_L					12.2	7.9K
40D		k_S	2.6K	2.6K	5.2K	OOM	55.7	2.6K
		k_L					0.45	2.6K
VISMALE 7D	V-RIPS	k_S	134	152	286	9.9K	7.38	142
		k_L					4.54	139
FOOT 10D		k_S	2.1K	2.1K	4.2K	376K	65.1	2.2K
		k_L					11.5	2.1K
LUCY 34D		k_S	2.0K	2.1K	4.1K	2.1M$^\times$	86.2	2.1K
		k_L					19.0	2.1K

Table 3: Storage costs, expressed in *megabytes*, of the several data structures on experimental datasets.

(ii) adjacency relation $R_{k,k}(\sigma)$ for each top CP k-cell σ;
(iii) co-boundary relation $R_{k-1,k}(\tau)$ for each non-manifold (k-1)-cell τ bounding a top CP k-cell;
(iv) partial co-boundary relation $R^*_{0,k}(v)$ for each vertex v. This consists of one arbitrarily selected top CP k-cell from each *k-cluster* in the star of v, where a k-cluster is a $(k-2)$-connected component of the link of v.

The Simplex tree encodes all j-simplices in Σ, with $0 \leq j \leq d$, and each block in the tree represents a vertex index. Each simplex σ is uniquely represented as an ordered path in the trie whose nodes correspond to the boundary vertices of σ. Thus, the nodes of the tree are in bijection with the simplices of the complex, and a Simplex tree over a simplicial complex with $|\Sigma|$ simplices (of any dimension) contains exactly $|\Sigma|$ nodes. We compare the Stellar tree to the implementation provided in [GUDHI, 2016], where each node of a Simplex tree requires 3 references to the tree structure (one pointer to the parent node, one pointer to the first of the children and one pointer to the next sibling node) and a reference to the label of the vertex, for a total of $4|\Sigma|$ references. We note that this implementation only supports the efficient extraction of boundary relations. An implementation that supports extraction of co-boundary and adjacency relations (as defined in [Boissonnat and Maria, 2014]) would require additional storage.

The Stellar tree and the IA* data structure can both represent CP complexes in arbitrary dimensions and thus the two structures have the same expressive power. Conversely, the Simplex tree can represent only simplicial complexes in arbitrary dimensions. A difference between the Stellar tree and the other two data structures is that the Stellar tree requires that the complex must be embedded in a space $\mathbb{E}^n$, while the other data structures are purely topological and do not require a spatial embedding.

We now consider the storage requirements for the different data structures (cf. Table 3). In 3D we consider triangle, tetrahedral, quad and hexahedral meshes, while in arbitrary dimensions we evaluate the storage costs on probabilistic-refinement models and Vietoris-Rips complexes. The analysis compares the topological overhead of the data structures, and thus, we omit the cost of the geometry of the underlying complex, which is common to all the data structures. For the Stellar tree we consider the full connectivity requirements, i.e., we consider both the hierarchy $\mathbb{H}$ and the boundary relation $R_{k,0}$ from the base mesh (see column *tot* in Table 3).

We can note that the Stellar tree is always more compact than the IA* data structure, requiring, on average, *half* of the storage on triangles, quads, tetrahedral meshes, probabilistic-refinement datasets and on V-Rips complexes, and from 40% to 50% less storage on *hexahedral* meshes. Considering now the *connectivity* storage costs, i.e., the storage required by the hierarchical structure $\mathbb{H}$ for the Stellar tree (see column *index* in Table 3) and the cost to encode the co-boundary and adjacencies relations in the IA* data structure (see column *conn*. in Table 3), we can note that the Stellar tree requires, with the used k_V values, a small fraction of the storage required by the IA* data structure, saving, in general, from 90% to 99% of the storage and from 80% to 99% on *hexahedral* datasets.

Comparing now the Stellar tree with respect to the Simplex tree, we can observe that the Stellar tree is always more compact, requiring from 65% to 80% less storage on 3D models, and from 85% to 99% less storage on the higher dimensional ones. We can observe how the storage requirements of the Simplex tree degenerate as the complex dimension increases.

These results confirm that the Stellar tree can efficiently represent non-manifold complexes in higher dimensions, with only a slight overhead relative to that of the indexed base mesh. This is largely due to the Stellar tree's exploitation and SRE compression of the complex's spatial locality.

8 General application paradigm

An advantage of the Stellar tree data structure is that it enables one to defer decisions about the details of the local topological data structure. Thus, one can easily customize the structure and layout of the representation to better suit the application.

We note that processing individual mesh elements in a Stellar tree representation can be expensive due to the compressed leaf block format. For example, to reconstruct the star of a given vertex v, we must first identify the leaf block b indexing v, and then visit the top cell lists in b to identify those that are incident in v. To amortize the reconstruction costs, we adopt a *batched* processing strategy for Stellar tree applications, in which we locally reconstruct

and process local subsets of the complex. This tends to work well in practice since mesh processing applications are often applied to the entire complex or to spatially coherent *regions of interest*.

The general paradigm for executing applications on the Stellar tree is to iterate through the leaf blocks of the hierarchy $\mathbb{H}$, locally processing the encoded complex in a streaming manner. For each leaf block b in $\mathbb{H}$, we construct a local topological data structure catered to the application and use to process the local complex. We refer to this local data structure as an *expanded leaf-block representation* b_E. Once we finish processing the leaf block b, we can discard b_E and begin processing the next block.

For efficiency and at relatively low storage overhead, we can cache the expanded leaf block representation b_E, using, e.g., a *Least-Recent-Used (LRU)* cache. This can be especially advantageous in applications that require processing portions of the complex in neighboring leaf block b. Adopting a fixed size cache allows us to amortize the extraction of the local data structures, with a controllable storage overhead.

Algorithm 4 shows the general paradigm for executing an application on the Stellar tree. The algorithm recursively visits all the blocks of the hierarchy $\mathbb{H}$. If block b is internal, we recursively call the procedure on b's children blocks. Otherwise, b is a leaf block, so we either recover b_E from the *LRU* cache (rows 5–10) or construct the desired application-dependent local topological data structure b_E. After using this local data structure to process the local geometry in b (row 9), we either cache or discard b_E (rows 10–13).

We distinguish between applications executed on a Stellar tree based on a *local* or a *global* approach. In the former, the scope of auxiliary variables and data structures is limited to that of a single leaf block b, or to a restricted subset of its neighbors. In the latter, auxiliary variables are maintained globally (outside the scope of a leaf block b) as we process the complex. In general, the local approach is preferred for applications that extract or analyze local features, while the global approach is preferred for applications that extract or analyze global features. Examples of the former include those that depend on the link or star of mesh elements or on the gradient of a scalar field defined on the vertices of the complex. Examples of the latter include geometric simplification or morphological feature analysis.

Algorithm 4 STELLAR_TREE_APPLICATION

Require: b is a block in $\mathbb{H}$
Require: *cache* is a fixed-size *LRU*-cache
1: **if** $b \in \mathbb{H}_I$ **then**
2: **for all** blocks c in CHILD(b) **do**
3: STELLAR_APPLICATION(c,*cache*)
4: **else** // $b \in \mathbb{H}_L$ //
5: **if** *cache*.HAS_IN(b) **then** // *expanded* b_E *is in cache*
6: $b_E \leftarrow$ *cache*.GET(b)
7: **else**
8: $b_E \leftarrow$ expand b representation
9: execute application using b_E
10: **if** *cache*.MAX_SIZE() > 0 **then** // *we use a cache* //
11: save b_E in *cache*
12: **else**
13: discard b_E

The decision between using a local and global approach involves a tradeoff between minimizing memory and execution times. Due to the limited scope of auxiliary data structures in the local approach, the storage overhead is typically proportional to the complexity of the local complex. However, this strategy leads to an increased number of memory allocations relative to a global approach since each leaf block expansion requires memory allocations. Conversely, while the auxiliary data structures in the global approach are allocated only once, these structures can require significantly more storage space compared to the local approach.

9 Current Developments

Currently, we are extensively experiment the Stellar tree on several applications, such as:

1. the extraction of individual topological relations, focusing on the more interesting co-boundary and adjacency relations;
2. the generation of existing state of the art topological data structures, such as the half-edge data structure over polynomial complexes and adjacency based data structures of manifold (IA) and non-manifold (IA*) CP complexes;

Topological queries are the key building blocks for locally traversing and processing the underlying complex. Co-boundary queries are naturally supported by the Stellar decomposition model. By definition, all regions of the decomposition that contain at least one vertex of a CP

cell τ must index all CP cells in the star of τ (see Equation 1). Since the top cells are explicitly represented in Σ, the key topological relations to extract is the the vertex co-boundary relation $R_{0,k}$ restricted to the top k-cells of Σ. The restricted vertex co-boundary relation $R_{0,k}$ in a leaf block b can be generated by inverting boundary relation $R_{k,0}$ on the top CP k-cells in $\Phi_{TOP}(b)$. Since the indexed vertices in the leaf blocks of a COMPRESSED Stellar tree are contiguous, with indices in the range $[v_{start}, v_{end})$, we encode our local data structure using an array of size $|\Phi_{VERT}(b)| = v_{end} - v_{start}$. Each position in the array corresponds to a vertex indexed by b and points to an (initially empty) list of indexes from Σ_T. We populate these arrays by iterating through relation $R_{k,0}$ of the top CP k-cells in $\Phi_{TOP}(b)$. For each cell σ whose boundary relation $R_{k,0}(\sigma)$ has a vertex with index $i_v \in [v_{start}, v_{end})$, we add the index of σ to vertex v's list. All the other co-boundary relations are just a specialization of the restricted vertex co-boundary.

The efficient extraction of topological relations is required for the generation of topological data structures within the Stellar tree. In our current developments we are considering two popular topological mesh data structures over CP complexes: the *half-edge* data structure over polygonal 2-manifolds and the *IA** data structure over non-manifold CP complexes in arbitrary dimension. These two applications demonstrate the versatility of the Stellar tree representation and exercise many of the operations necessary for other mesh processing tasks. In both cases, we define customized topological relations and auxiliary data structures as we stream through the leaf blocks of the tree and take either a *global* approach, to reconstruct the full topological data structure, or a *local* approach, which reconstructs coherent subsets of the full data structure restricted to the portion of the complex indexed within each leaf block. In the former case, Stellar trees enable generating the global topological data structures using a fraction of the memory as would be required to directly generate from an indexed representation. In the latter case, the local approach can be used to adapt local regions of the Stellar tree's underlying complex to algorithms defined for existing topological data structures.

Acknowledgments

This work has been partially supported by the National Science Foundation under grant number IIS-1116747. It has also been performed under the auspices of the U.S. Department of Energy by Lawrence Livermore National Laboratory under contract DE-AC52-07NA27344.

Datasets are courtesy of *Volvis* repository (BONSAI, F16 and FOOT), the *Volume Library* (*volib*) (VISMALE), *CMU Unstructured Mesh Suite* (SAN FERNANDO) and *Aim@Shape* repository (NEPTUNE, STATUETTE and LUCY).

References

[Attali et al., 2012] Attali, D., Lieutier, A., and Salinas, D. (2012). Efficient data structure for representing and simplifying simplicial complexes in high dimensions. *International Journal of Computational Geometry & Applications*, 22(04):279–303.

[Bentley, 1975] Bentley, J. (1975). Multidimensional binary search trees used for associative searching. *Communications of the ACM*, 18(9):509–517.

[Boissonnat and Maria, 2014] Boissonnat, J.-D. and Maria, C. (2014). The simplex tree: An efficient data structure for general simplicial complexes. *Algorithmica*, 70(3):406–427.

[Canino and De Floriani, 2014] Canino, D. and De Floriani, L. (2014). Representing simplicial complexes with Mangroves. In *Proceedings of the 22nd International Meshing Roundtable*, pages 465–483. Springer.

[Canino et al., 2011] Canino, D., De Floriani, L., and Weiss, K. (2011). IA*: An adjacency-based representation for non-manifold simplicial shapes in arbitrary dimensions. *Computers & Graphics*, 35(3):747–753.

[Carlbom et al., 1985] Carlbom, I., Chakravarty, I., and Vanderschel, D. (1985). A hierarchical data structure for representing the spatial decomposition of 3d objects. *IEEE Computer Graphics and Applications*, 5(4):24–31.

[Cignoni et al., 2003a] Cignoni, P., Ganovelli, F., Gobbetti, E., Marton, F., Ponchio, F., and Scopigno, R.

(2003a). BDAM – Batched Dynamic Adaptive Meshes for high performance terrain visualization. *Computer Graphics Forum*, 22(3):505–514.

[Cignoni et al., 2004] Cignoni, P., Ganovelli, F., Gobbetti, E., Marton, F., Ponchio, F., and Scopigno, R. (2004). Adaptive tetrapuzzles: Efficient out-of-core construction and visualization of gigantic multiresolution polygonal models. *ACM Transactions on Graphics*, 23(3):796–803.

[Cignoni et al., 2003b] Cignoni, P., Montani, C., Rocchini, C., and Scopigno, R. (2003b). External memory management and simplification of huge meshes. *IEEE Transactions on Visualization and Computer Graphics*, 9(4):525–537.

[Damiand and Lienhardt, 2014] Damiand, G. and Lienhardt, P. (2014). *Combinatorial Maps: Efficient Data Structures for Computer Graphics and Image Processing*. CRC Press.

[De Floriani et al., 2008] De Floriani, L., Facinoli, M., Magillo, P., and Dimitri, D. (2008). A hierarchical spatial index for triangulated surfaces. In *Proceedings of the Third International Conference on Computer Graphics Theory and Applications (GRAPP 2008)*, pages 86–91.

[De Floriani et al., 2010] De Floriani, L., Fellegara, R., and Magillo, P. (2010). Spatial indexing on tetrahedral meshes. In *Proceedings of the 18th SIGSPATIAL International Conference on Advances in Geographic Information Systems*, pages 506–509. ACM.

[De Floriani et al., 2004] De Floriani, L., Greenfieldboyce, D., and Hui, A. (2004). A data structure for non-manifold simplicial d-complexes. In *Proceedings of the 2004 Eurographics/ACM SIGGRAPH symposium on Geometry processing*, pages 83–92. ACM.

[De Floriani and Hui, 2005] De Floriani, L. and Hui, A. (2005). Data structures for simplicial complexes: An analysis and a comparison. In *Proceedings of the third Eurographics symposium on Geometry processing*, pages 119–es. Eurographics Association.

[De Floriani et al., 2010] De Floriani, L., Hui, A., Panozzo, D., and Canino, D. (2010). A dimension-independent data structure for simplicial complexes. *Proceedings of the 19th International Meshing Roundtable*, pages 403–420.

[Dey et al., 2010] Dey, T., Levine, J., and Slatton, A. (2010). Localized delaunay refinement for sampling and meshing. *Computer Graphics Forum*, 29(5):1723–1732.

[Edelsbrunner, 1987] Edelsbrunner, H. (1987). *Algorithms in combinatorial geometry*, volume 10. Springer Verlag.

[Fellegara et al., 2014] Fellegara, R., Iuricich, F., De Floriani, L., and Weiss, K. (2014). Efficient computation and simplification of discrete Morse decompositions on triangulated terrains. In *Proceedings of the 22th ACM SIGSPATIAL International Conference on Advances in Geographic Information Systems*. ACM.

[Fredkin, 1960] Fredkin, E. (1960). Trie memory. *Communications of the ACM*, 3(9):490–499.

[Fugacci et al., 2015] Fugacci, U., Iuricich., F., and De Floriani, L. (2015). Homology computation in higher dimensions based on discrete morse theory. In *in preparation*.

[GUDHI, 2016] GUDHI (2016). Geometric understanding in higher dimensions (GUDHI). `https://project.inria.fr/gudhi/` [Online; accessed 06-March-2016].

[Gurung and Rossignac, 2009] Gurung, T. and Rossignac, J. (2009). SOT: A compact representation for tetrahedral meshes. In *Proceedings SIAM/ACM Geometric and Physical Modeling*, SPM '09, pages 79–88, San Francisco, USA.

[Held and Marshall, 1991] Held, G. and Marshall, T. (1991). *Data compression; techniques and applications: Hardware and software considerations*. John Wiley & Sons.

[Hunter and Willis, 1991] Hunter, A. and Willis, P. (1991). Classification of quad-encoding techniques. In *Computer Graphics Forum*, volume 10, pages 97–112.

[Lawson, 1977] Lawson, C. L. (1977). Software for C^1 surface interpolation. In Rice, J., editor, *Mathematical Software III*, pages 161–194. Academic Press.

[Lienhardt, 1994] Lienhardt, P. (1994). N-dimensional generalized combinatorial maps and cellular quasi-manifolds. *International Journal of Computational Geometry and Applications*, 4(3):275–324.

[Mantyla, 1988] Mantyla, M. (1988). *An Introduction to Solid Modeling*. Computer Science Press.

[MTDSL, 2014] MTDSL (2014). Mangrove topological data structure library. `http://mangrovetds.sourceforge.net/` [Online; accessed 02-March-2015].

[Nabutovsky, 1996] Nabutovsky, A. (1996). Geometry of the space of triangulations of a compact manifold. *Communications in mathematical physics*, 181(2):303–330.

[Navazo, 1989] Navazo, I. (1989). Extended octree representation of general solids with plane faces: Model structure and algorithms. *Computer & Graphics*, 13(1):5–16.

[Nielson, 1997] Nielson, G. M. (1997). Tools for triangulations and tetrahedralizations and constructing functions defined over them. In Nielson, G. M., Hagen, H., and Müller, H., editors, *Scientific Visualization: overviews, Methodologies and Techniques*, chapter 20, pages 429–525. IEEE Computer Society, Silver Spring, MD.

[Paoluzzi et al., 1993] Paoluzzi, A., Bernardini, F., Cattani, C., and Ferrucci, V. (1993). Dimension-independent modeling with simplicial complexes. *ACM Transactions on Graphics (TOG)*, 12(1):56–102.

[Poirier et al., 1998] Poirier, D., Allmaras, S., McCarthy, D., Smith, M., and Enomoto, F. (1998). The CGNS system. *AIAA Fluid Dynamics Conference*.

[Remacle and Shephard, 2003] Remacle, J. F. and Shephard, M. S. (2003). An algorithm oriented mesh database. *International Journal for Numerical Methods in Engineering*, 58(2):349–374.

[Rossignac et al., 2001] Rossignac, J., Safonova, A., and Szymczak, A. (2001). 3D compression made simple: Edge-Breaker on a Corner Table. In *Proceedings Shape Modeling International 2001*, Genova, Italy. IEEE Computer Society.

[Samet, 2006] Samet, H. (2006). *Foundations of Multidimensional and Metric Data Structures*. Morgan Kaufmann.

[Samet and Webber, 1985] Samet, H. and Webber, R. (1985). Storing a collection of polygons using quadtrees. *ACM Transactions on Graphics (TOG)*, 4(3):182–222.

[Schoof and Yarberry, 1994] Schoof, L. A. and Yarberry, V. R. (1994). EXODUS II: A finite element data model. Technical Report SAND92-2137, Sandia National Laboratories, Albuquerque, NM.

[Tautges, 2010] Tautges, T. J. (2010). Canonical numbering systems for finite-element codes. *International Journal for Numerical Methods in Biomedical Engineering*, 26(12):1559–1572.

[Weiss and De Floriani, 2011] Weiss, K. and De Floriani, L. (2011). Simplex and diamond hierarchies: Models and applications. *Computer Graphics Forum*, 30(8):2127–2155.

[Weiss et al., 2011] Weiss, K., Fellegara, R., De Floriani, L., and Velloso, M. (2011). The PR-star octree: A spatio-topological data structure for tetrahedral meshes. In *Proceedings of the 19th ACM SIGSPATIAL International Conference on Advances in Geographic Information Systems*, pages 92–101. ACM.

[Weiss et al., 2013] Weiss, K., Iuricich, F., Fellegara, R., and De Floriani, L. (2013). A primal/dual representation for discrete Morse complexes on tetrahedral meshes. In *Computer Graphics Forum*, volume 32, pages 361–370.

[Zomorodian, 2010] Zomorodian, A. (2010). Fast construction of the Vietoris-Rips complex. *Computers & Graphics*, 34(3):263–271.